J. Phys. B: At. Mol. Opt. Phys. **32** (1999) 1523–1534. Printed in the UK PII: S0953-4075(99)98104-X

Ab initio study of charge transfer in low-energy Si^{3+} collisions with helium

P C Stancil†¶, N J Clarke‡[+], B Zygelman§* and D L Cooper‖[#]

† Physics Division, Oak Ridge National Laboratory, PO Box 2008, Oak Ridge, TN 37831-6372, USA

‡ School Of Chemistry, University Of Birmingham, Edgbaston, Birmingham B15 2TT, UK

§ Institute for Theoretical Atomic and Molecular Physics, Harvard–Smithsonian Center for Astrophysics, 60 Garden St., Cambridge, MA 02138, USA

‖ Department of Chemistry, University of Liverpool, PO Box 147, Liverpool L69 7ZD, UK

Received 5 October 1998, in final form 27 January 1999

Abstract. Charge transfer cross sections for collisions of ground state $Si^{3+}(3s\,^2S)$ and excited state $Si^{3+}(3p\,^2P^o)$ with atomic helium are presented for energies less than 250 eV u^{-1}. Using a fully quantum mechanical, molecular-orbital, close-coupling approach, the cross sections are calculated in a diabatic representation. Completely *ab initio* adiabatic potentials and nonadiabatic radial coupling matrix elements obtained with the spin-coupled valence-bond method are utilized. Rate coefficients for temperatures between 100 and 100 000 K and cross sections for collisions with isotopic ^3He are presented. Results for the reverse process, $Si^{2+} + He^+$, are also given.

1. Introduction

The charge transfer processes

$$Si^{3+}(3s\,^2S) + He(1s^2) \rightarrow Si^{2+}(3s^2\,^1S) + He^+(1s), \quad (1)$$

$$\rightarrow Si^{2+}(3s3p\,^3P^o) + He^+(1s), \quad (2)$$

are important recombination mechanisms for Si^{3+} in gaseous nebulae. Reaction (1) has been shown by Baliunas and Butler (1980) and Butler and Raymond (1980) to be crucial for establishing the ionization balance of coronal plasmas and low-velocity shocked regions. The reaction has been previously investigated by Butler and Dalgarno (1980) using the Landau–Zener approximation and with a quantal close-coupling approach by Honvault *et al* (1998). The only experimental information is available from a rate coefficient measurement at 3900 K by Fang and Kwong (1997).

In this paper, we present an *ab initio* investigation of processes (1) and (2) in which the scattering equations are solved in a diabatic representation through a fully quantum mechanical, molecular-orbital, close-coupling (MOCC) approach (see, for example, Zygelman *et al* 1992). We include only radial coupling as rotational coupling is expected to give a negligible

¶ Eugene P Wigner Fellow. E-mail address:stancil@mail.phy.ornl.gov

[+] E-mail address: nickc@tcpc.bham.ac.uk

* Permanent address: Department of Physics, University of Nevada, Las Vegas, NV 89154-4002, USA. E-mail address:bernard@physics.unlv.edu

[#] E-mail address: dlc@rs2.ch.liv.ac.uk

0953-4075/99/061523+12$19.50

Table 1. Asymptotic separated-atom energies for the $^2\Sigma^+$ states of $SiHe^{3+}$.

Molecular state	Asymptotic atomic states	Energy (eV)		
		Theory[a]	Theory[b]	Expt[c]
$1\,^2\Sigma^+$	$Si^{2+}(3s^2\,^1S) + He^+(1s)$	− 8.874	−8.606	−8.906
$2\,^2\Sigma^+$	$Si^{2+}(3s3p\,^3P^o) + He^+(1s)$	−2.499	−2.214	−2.336
$3\,^2\Sigma^+$	$Si^{3+}(3s\,^2S) + He(1s^2)$	0.0	0.0	0.0
$4\,^2\Sigma^+$	$Si^{2+}(3s3p\,^1P^o) + He^+(1s)$	1.622	1.834	1.371
$^2\Sigma^+$	$Si^{2+}(3p^2\,^1D) + He^+(1s)$	—	—	6.247
$^2\Sigma^+$	$Si^{2+}(3s3d\,^3D) + He^+(1s)$	—	—	8.817
$5\,^2\Sigma^+$	$Si^{3+}(3p\,^2P^o) + He(1s^2)$	8.906	8.781	8.876

[a] This work.
[b] Honvault *et al* (1998).
[c] Bashkin and Stoner (1975).

contribution in the low-energy regime. We further investigate the isotope dependence for ^{3}He targets, present an analysis of electron capture processes for the $Si^{3+}(3p\,^2P^o)$ excited state,

$$Si^{3+}(3p\,^2P^o) + He(1s^2) \rightarrow Si^{2+}(3s3p\,^1P^o) + He^+(1s), \quad (3)$$

$$\rightarrow Si^{2+}(3s3p\,^3P^o) + He^+(1s), \quad (4)$$

$$\rightarrow Si^{2+}(3s^2\,^1S) + He^+(1s), \quad (5)$$

and present cross sections for the reverse process, $Si^{2+} + He^+$. Atomic units are used throughout unless otherwise noted.

2. Electronic structure calculations

Adiabatic potentials and radial coupling matrix elements are obtained using the spin-coupled valence-bond (SCVB) approach. The basic strategy is very similar to that described in our previous work (see, for example, Cooper, Gerratt and Raimondi 1988) and so we indicate here only those features that are particularly salient to the present study. Further details can be found elsewhere (Clarke 1995, Clarke and Cooper 1998).

We adopt Dunning correlation-consistent basis sets of triple-ζ-valence quality for Si/He consisting of (15s9p2d/6s2p) Cartesian Gaussian-type orbitals contracted to (5s4p2d/3s2p). SCVB expansions are performed in the space of the three valence electrons, with the $Si(1s^22s^22p^6)$ core described by (optimized) molecular orbitals taken from appropriate state-averaged, full-valence complete-active-space self-consistent field (CASSCF) calculations (Clarke 1995). All single and double vertical excitations plus singly-ionic cross excitations are included into the chosen set of virtual orbitals. The latter consists of three σ and two π pairs of virtuals for each valence electron, plus an additional δ pair for each of the $Si^{2+}(3s)$ electrons. The final very compact SCVB wavefunctions consist of just 154 spatial configurations (234 VB structures). The calculations are carried out for 47 nuclear separations R from 2.0–14 au.

The resulting adiabatic potential energies are displayed in figure 1. Table 1 presents the calculated and experimental separated-atom energies relative to the neutral incoming ground Si^{3+} channel. The deviation of the current results from the experimental energies is less than $\sim$0.16 eV, except for the $4\,^2\Sigma^+$ channel (0.25 eV) which plays an insignificant role in charge transfer from the Si^{3+} ground state, and are generally in better agreement with experiment than the CIPSI (configuration interaction by perturbation of a multiconfiguration wavefunction selected iteratively) energies of Honvault *et al* (1998). For the dominant capture channel, $1\,^2\Sigma^+$, our absolute energy error is only 0.03 eV while that of Honvault *et al* was 0.30 eV.

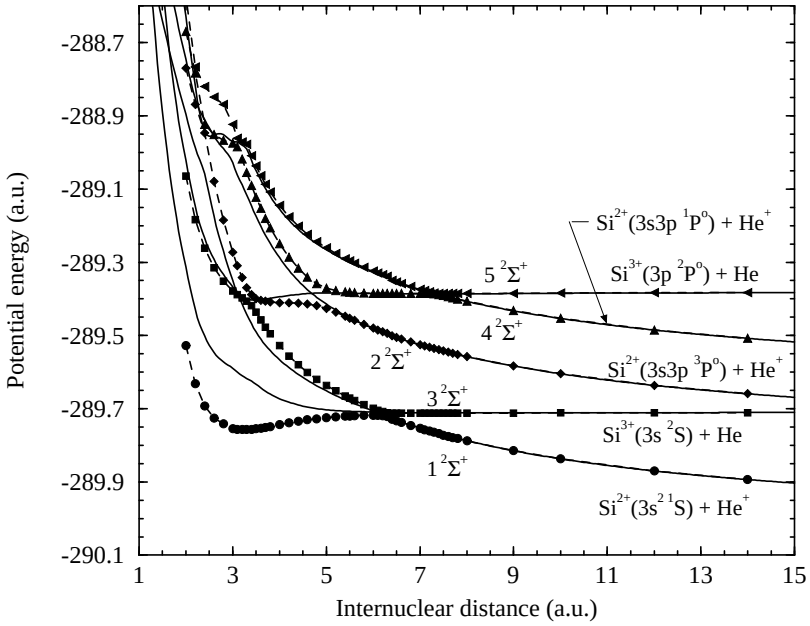

Figure 1. The $^2\Sigma^+$ adiabatic (- - - - with symbols) and diagonal diabatic (——) potential energies for the $SiHe^{3+}$ system as a function of internuclear distance R.

We do not consider the states correlating to $Si^{2+}(3p^2\ ^1D)$ + He^+ and $Si^{2+}(3s3d\ ^3D)$ + He^+ as they are endoergic by 6.2 and 8.8 eV, respectively, for capture from $Si^{3+}(3s\ ^2S)$ and have avoided crossings with the $Si^{3+}(3p\ ^2P^o)$ channel near $R_x \sim 21$ and ∼900 au, respectively. These channels are expected to give negligible contributions to the charge transfer cross sections for the considered collision energies. We also neglected the double electron capture channel, $Si^+(3s^2 3p\ ^2P^o)$ + He^{2+}, which should have an inconsequential cross section as it is endoergic by 30 and 21 eV for capture from $Si^{3+}(3s\ ^2S)$ and $Si^{3+}(3p\ ^2P^o)$, respectively.

The avoided crossing distances R_x and the corresponding energy differences $\Delta U(R_x)$ are listed in table 2 for the empirical potentials of Butler and Dalgarno (1980), the CIPSI potentials of Honvault *et al* (1998) and the present SCVB potentials. The positions of the avoided crossings and the $\Delta U(R_x)$ are in fair agreement with those obtained by Honvault *et al*.

Selected radial couplings (matrix elements of $\partial/\partial R$) are illustrated in figure 2. The peaks corresponding to the avoided crossings are smooth, well defined and centred directly on the positions of the crossings. The couplings between non-adjacent states (not shown) are much smaller than those between adjacent states as expected. However, we currently have no absolute criterion for assigning phases to the radial couplings. Phase changes are imposed when matrix elements otherwise approached zero with a gradient sufficient to introduce discontinuities. The current radial couplings are very similar to those of Honvault *et al* (1998), except that our peak values are generally larger.

Given the nonadiabatic couplings, we transform to a diabatic representation by a unitary transformation to eliminate first-order derivatives (see, for example, Zygelman *et al* 1992). The diagonal elements of the resulting diabatic potential matrix are displayed in figure 1 while the off-diagonal elements are given in figure 3.

Table 2. Avoided crossings and adiabatic potential differences at avoiding crossings for the $^2\Sigma^+$ states of $SiHe^{3+}$.

Molecular states	R_x (au)	ΔU_x (eV)
$1\,^2\Sigma^+$–$3\,^2\Sigma^+$	6.1[a]	0.282[a]
	6.0[b]	0.25[b]
	6.3[c]	0.270[c]
$2\,^2\Sigma^+$–$3\,^2\Sigma^+$	3.2[b]	0.707[b]
	3.4[c]	0.795[c]
$2\,^2\Sigma^+$–$4\,^2\Sigma^+$	4.9[b]	1.570[b]
	5.0[c]	1.525[c]
$4\,^2\Sigma^+$–$5\,^2\Sigma^+$	7.0[b]	0.054[b]
	7.3[c]	0.051[c]

[a] From empirical potentials obtained using procedures of Butler and Dalgarno (1980).
[b] From CIPSI potentials of Honvault *et al* (1998).
[c] From *ab initio* potentials, this work.

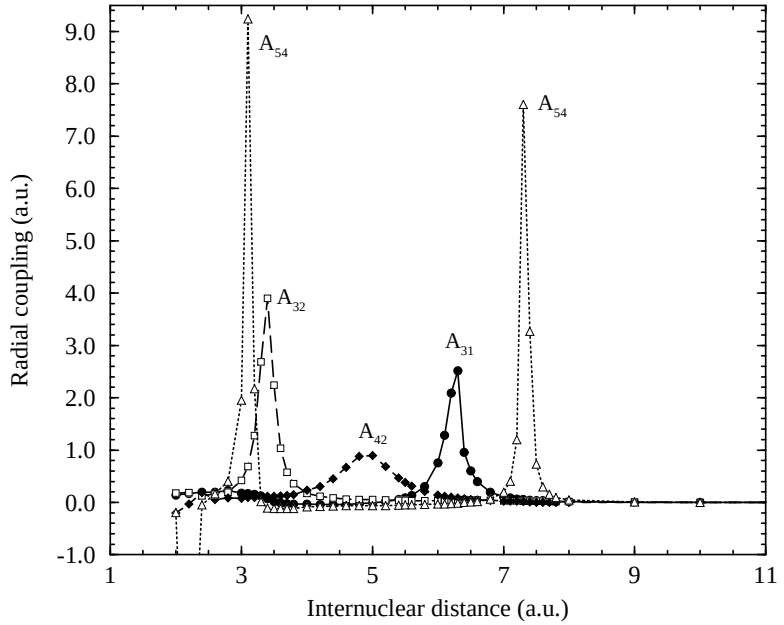

Figure 2. Selected $^2\Sigma^+$ nonadiabatic radial couplings for the $SiHe^{3+}$ system as a function of internuclear distance R.

3. Results and discussion

The calculations are performed in the perturbed-stationary-state approximation using a fully quantum mechanical MOCC approach previously described in Zygelman *et al* (1992) where the coupled scattering equations are integrated using an implementation of the log-derivative method of Johnson (1973). All five channels are included except when the incident collision energy is such that the $2\,^2\Sigma^+$, $4\,^2\Sigma^+$ and $5\,^2\Sigma^+$ channels are closed, in which case a two-channel calculation is performed.

The cross sections were computed on a fine collision energy grid of typically 20–30

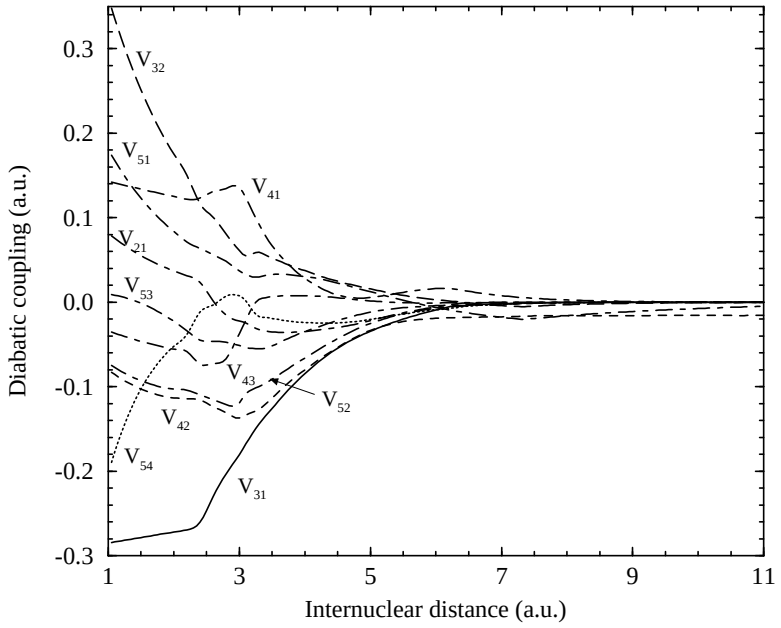

Figure 3. The $^2\Sigma^+$ off-diagonal diabatic potentials for the $SiHe^{3+}$ system as a function of internuclear distance R.

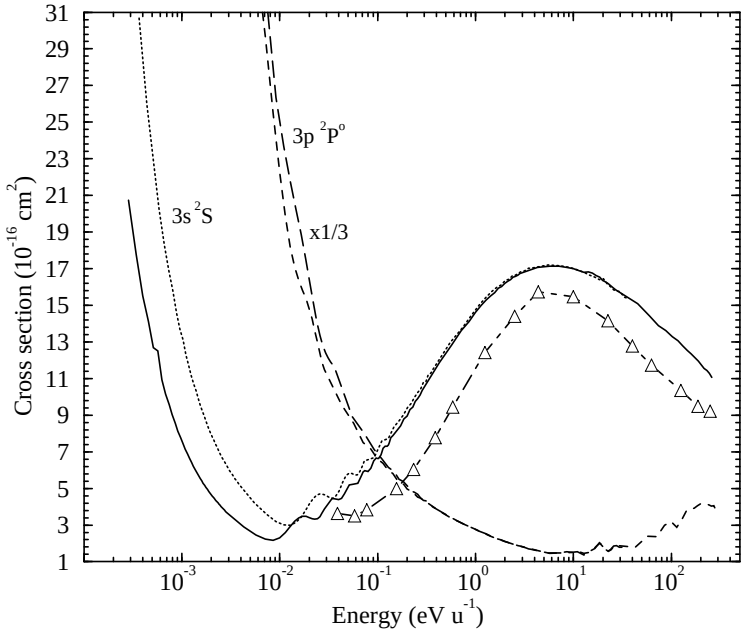

Figure 4. Total electron capture cross sections. This work, $Si^{3+}(3s\,^2S)$ + ^4He (——), $Si^{3+}(3s\,^2S)$ + ^3He (· · · · · ·), $Si^{3+}(3p\,^2P^o)$ + ^4He (- - - -), and $Si^{3+}(3p\,^2P^o)$ + ^3He (– – –). Honvault *et al* (1998), $Si^{3+}(3s\,^2S)$ + ^4He (— · — with triangles). Note that the $3p\,^2P^o$ cross sections have been multiplied by $\frac{1}{3}$.

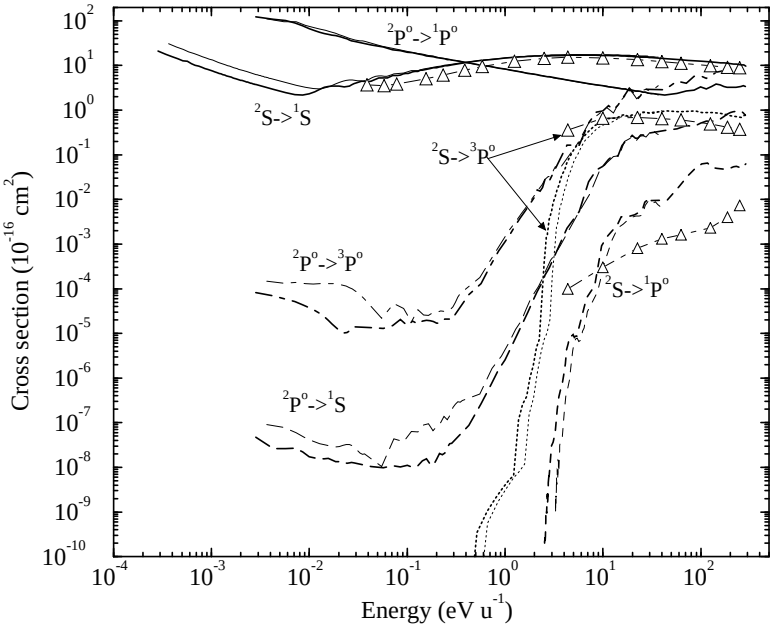

Figure 5. State-selective electron capture cross sections with ^{4}He (thick curves) and ^{3}He (thin curves) targets. The initial Si^{3+} and final Si^{2+} states are indicated in the figure and the energy scale refers to the centre-of-mass collision energy in the entrance channel. Honvault *et al* (1998), ^{4}He (— · — with triangles).

points per decade and the numerical data can be obtained from the authors upon request. The conspicuous bumps and undulations evident in the cross section for capture by the ground state (figure 4), as well as other cross sections (figures 4, 5, and 8), represent the true behaviour of our numerical results. The regular oscillations in the $3s\,^2S$ cross section between $\sim 10^{-2}$ and 0.2 eV u^{-1} shown in figure 4 are a type of Stuckelberg oscillation (see, for example, Zygelman *et al* 1992), while the undulations in a number of other cross sections for energies above 10 eV u^{-1} are related to multichannel interference effects.

Electron translation factors (ETFs), which are often included to remove asymptotic couplings between atomic states that are connected by dipole transitions, are not included. For the current system, the $1\,^2\Sigma^+$ and $2\,^2\Sigma^+$ states and the $2\,^2\Sigma^+$ and $4\,^2\Sigma^+$ states are dipole-coupled through weak intercombination dipole moments, the former with a strength of $\sim 0.01\ ea_0$. While the asymptotic dipole moments coupling the $1\,^2\Sigma^+$ and $4\,^2\Sigma^+$ states and the $3\,^2\Sigma^+$ and $5\,^2\Sigma^+$ states are strong, neglect of ETFs is expected to have a negligible effect for the currently investigated energy range. The initial channel approach probability, or degeneracy, factors are explicitly included in all presented cross sections and rate coefficients.

3.1. Electron capture from the $Si^{3+}(3s^2\,^1S)$ ground state

Charge transfer cross sections for the sum of process (1) and (2) are presented in figure 4 as a function of the centre-of-mass collision energy E divided by the nuclear reduced mass μ. The current results are in good agreement with the MOCC calculations of Honvault *et al* (1998), but typically larger by <40%. The discrepancy may be partially due to differences in the peak of the radial coupling A_{31}, for which the current value is 70% larger than that obtained by Honvault *et al*, and/or differences in the asymptotic energies.

Table 3. Charge transfer rate coefficients α ($cm^3\ s^{-1}$) for ^{4}He targets as a function of temperature T. Fitting parameters a_i ($cm^3\ s^{-1}$), b_i, and c_i(K) according to equation (6) are given at the end of the table. The notation $A - B$ corresponds to $A \times 10^{-B}$.

	Reaction			
T (K)	(1)	(2)	(3)	(4)
100	2.92–11	—	—	—
300	4.33–11	—	—	—
500	6.34–11	—	8.29–10	3.72–16
700	8.42–11	—	8.36–10	3.89–16
900	1.05–10	—	8.40–10	4.11–16
1 000	1.15–10	—	8.42–10	4.25–16
2 000	2.17–10	—	8.61–10	6.06–16
4 000	4.07–10	—	9.00–10	1.51–15
6 000	5.79–10	1.30–19	9.33–10	4.96–15
8 000	7.36–10	8.23–18	9.60–10	1.41–14
10 000	8.81–10	1.27–16	9.83–10	3.29–14
15 000	1.20–9	6.47–15	1.03–9	1.54–13
20 000	1.48–9	5.58–14	1.06–9	4.62–13
30 000	1.96–9	6.08–13	1.12–9	2.01–12
40 000	2.36–9	2.32–12	1.16–9	5.23–12
50 000	2.71–9	5.55–12	1.19–9	1.06–11
60 000	3.03–9	1.04–11	1.23–9	1.84–11
70 000	3.32–9	1.66–11	1.26–9	2.86–11
80 000	3.58–9	2.39–11	1.29–9	4.12–11
90 000	3.83–9	3.22–11	1.33–9	5.60–11
100 000	4.06–9	4.11–11	1.36–9	7.28–11
a_1	8.69–10	1.09–14	9.58–10	6.32–16
b_1	8.42–1	1.64+1	5.63–2	2.05–1
c_1	2.46+5	2.09+3	−4.24+5	−1.10+4
a_2	—	1.29–17	—	3.88–14
b_2	—	1.18+1	—	4.18
c_2	—	7.95+3	—	4.53+4

State-selective cross sections for capture into the $Si^{2+}(3s^2\ ^1S)$ (reaction 1), $Si^{2+}(3s3p\ ^3P^o)$ (reaction 2) and $Si^{2+}(3s3p\ ^1P^o)$ states are shown in figure 5. Since the $Si^{2+}(3s3p\ ^3P^o)$ channel has an avoided crossing of about $R_x \sim 23$ au and the $Si^{2+}(3s3p\ ^1P^o)$ channel is endoergic by 1.4 eV, both are unimportant for the considered energy range, but may contribute for higher energies. For ^{4}He targets, this corresponds to a $Si^{2+}(3s3p\ ^1P^o)$ threshold of 0.4 eV u^{-1} (0.5 eV u^{-1} for ^{3}He targets). The state-selective results of Honvault *et al* (1998) are also shown in figure 5 and are in fair agreement with the current calculations. The major discrepancy is for capture to the $Si^{2+}(3s3p\ ^1P^o)$ state which may be related to the larger asymptotic energy error of 0.46 eV of Honvault *et al* in comparison to the current error of 0.25 eV (see table 1). For reaction (2), the small discrepancy may be related to our larger radial coupling A_{32}. However, in both cases our neglect of rotational coupling may play some role in the differences.

In table 3, we present rate coefficients for the electron capture processes (1) and (2) which were determined by averaging over the cross sections with a Maxwellian velocity distribution. The rates are fitted to the parametric form

$$\alpha(T) = \sum_i a_i \left(\frac{T}{10\,000}\right)^{b_i} \exp\left(\frac{-T}{c_i}\right) \tag{6}$$

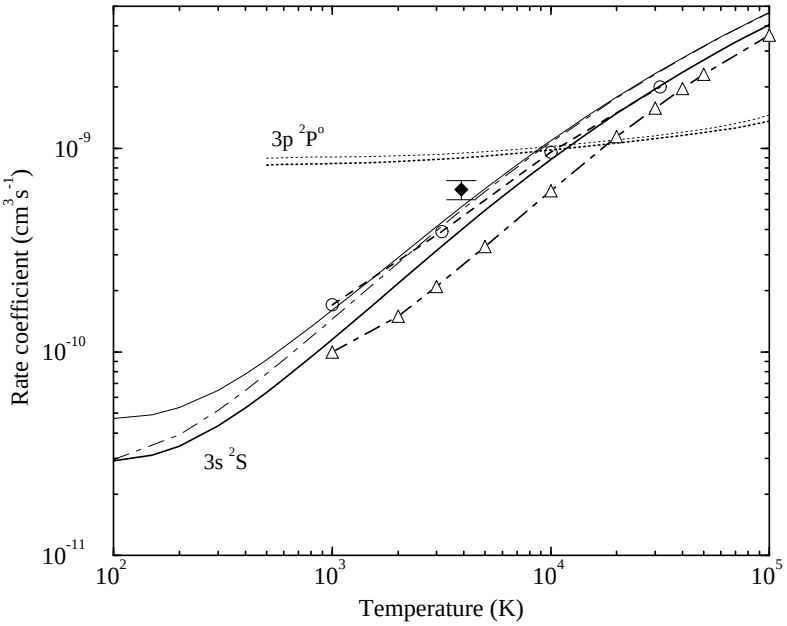

Figure 6. Total electron capture rate coefficients. $Si^{3+}(3s\,^2S + {}^4He$: this work (thick ——); Butler and Dalgarno (1980) (- - - - with circles); Honvault *et al* (1998) (— · — with triangles); and experiment, Fang and Kwong (1997) (filled diamond). This work: $Si^{3+}(3s\,^2S) + {}^3He$ with ^{3}He cross section (thin ——) and with mass-scaled ^{4}He cross section (— · —); $Si^{3+}(3s\,^2P^o) + {}^4He$ (thick · · · · · ·); and $Si^{3+}(3s\,^2P^o) + {}^3He$ (thin · · · · · ·).

with the parameters a_i (cm^3 s^{-1}), b_i, and c_i (K) given at the bottom of table 3. The fits are reliable to within 10% for $T > 200$ K, except for reaction (2) which is only accurate to within 40%. The current quantal rate coefficients, presented in figure 6, are in fair agreement with the Landau–Zener calculations of Butler and Dalgarno (1980) and the MOCC results of Honvault *et al* (1998), with the magnitude of the current values generally midway between the other two results. Our rate coefficient is about 40% smaller than the ^{4}He ion trap measurement of Fang and Kwong (1997) at 3900 K, which is in fact larger than the other previous calculations as well. The discrepancy may be due to an uncertainty in the equivalent temperature of the reactants in the trap. Merged-beams measurements in this energy regime would be desirable.

3.2. Target isotope dependence

The influence of an isotope effect on the total low-energy charge transfer cross section has been discussed by Stancil and Zygelman (1995) and demonstrated for a number of collision systems (Pieksma *et al* 1996, Stancil *et al* 1997a, b, Clarke *et al* 1998). From the Landau–Zener approximation, Stancil and Zygelman (1995) derived an expression to relate the thermal energy ^{3}He target and ^{4}He target cross sections:

$$\frac{\sigma(^3\mathrm{He})}{\sigma(^4\mathrm{He})} \approx \frac{1 - 2V_{ii}/\mu(^3\mathrm{He})v^2}{1 - 2V_{ii}/\mu(^4\mathrm{He})v^2} \tag{7}$$

where V_{ii} is the diabatic potential of the entrance channel, μ the reduced mass of the isotopic quasi-molecule, and v the collision velocity in the centre-of-mass frame. Equation (7) predicts a threshold for the isotope effect of $\sim$0.46 eV/u and $\sigma(^3\mathrm{He})/\sigma(^4\mathrm{He}) \sim 1.22$ at 0.01 eV u^{-1}.

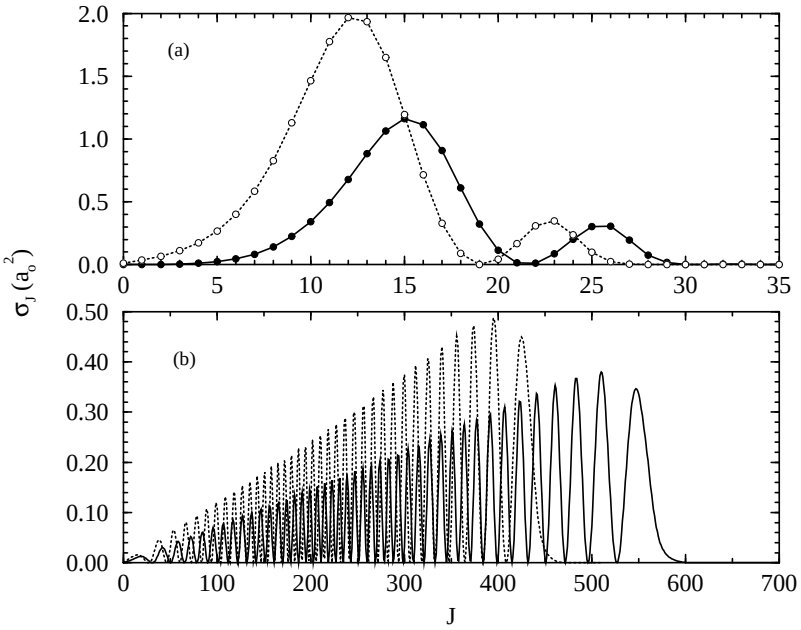

Figure 7. Partial cross sections σ_J versus J for capture into $Si^{2+}(3s^2\,{}^1S)$ from $Si^{3+}(3s\,{}^2S)$ + ^4He (——) and $Si^{3+}(3s\,{}^2S)$ + ^3He (· · · · · ·). (*a*) $E = 0.005$ eV u^{-1}, (*b*) $E = 5$ eV u^{-1}.

We define the threshold as the energy at which the ^{3}He target cross section is 2% larger than the ^{4}He target cross section. The quantum calculation, shown in figure 4, gives a threshold of $\sim$0.5 eV u^{-1} and $\sigma(^3\text{He})/\sigma(^4\text{He}) \sim 1.3$ at 0.01 eV u^{-1}.

State-selective cross sections for reactions (1) and (2) with ^{3}He targets are given in figure 5 while their rate coefficients are given in table 4 and figure 6. Also shown in figure 6 are the rate coefficients for ^{3}He targets, but calculated with the ^{4}He target cross section by scaling the collision energy with the reduced masses. The discrepancy reaches a maximum of 50% at 100 K.

Figure 7 presents partial cross sections σ_J versus total angular momentum J for reaction (1) with ^{4}He and ^{3}He targets at 0.005 and 5 eV u^{-1}. At 5 eV u^{-1}, the number of contributing partial waves for a ^{4}He target is about $\sim$25% more than for the ^{3}He target as shown in figure 7(*b*). However, the magnitude of the ^{4}He target partial cross sections are $\sim$25% smaller than the magnitude of the ^{3}He partial cross sections, with the net result of a target-mass-independent total cross section. For the lower collision energy of 0.005 eV u^{-1}, displayed in figure 7(*a*), the number of contributing partial cross sections for the ^{4}He target is again somewhat larger than that for the ^{3}He target. However, the maximum ^{3}He target partial cross section has nearly twice the magnitude of the maximum ^{4}He partial cross section, resulting in an enhanced total ^{3}He cross section. These target mass and J dependence behaviours are similar to those noted for other collision systems by Stancil *et al* (1997a, b) and Clarke *et al* (1998).

3.3. Electron capture from the $Si^{3+}(3p\,{}^2P^o)$ excited state

Cross sections for the charge transfer reactions (3) through (5) are presented in figure 5 and their sum in figure 4. The total cross section becomes greater than the $Si^{3+}(3s\,{}^2S)$ cross section for energies less than $\sim$0.4 eV/u. However, as the $Si^{3+}(3p\,{}^2P^o)$ is dipole connected to

Table 4. Charge transfer rate coefficients α (cm^3 s^{-1}) for ^{3}He targets as a function of temperature T. Fitting parameters a_i (cm^3 s^{-1}), b_i, and c_i(K) according to equation (6) are given at the end of the table. The notation $A-B$ corresponds to $A \times 10^{-B}$.

	Reaction			
T (K)	(1)	(2)	(3)	(4)
100	4.72–11	—	—	—
300	6.48–11	—	—	—
500	9.16–11	—	8.95–10	1.59–15
700	1.19–10	—	9.04–10	1.59–15
900	1.47–10	—	9.07–10	1.56–15
1 000	1.60–10	—	9.08–10	1.55–15
2 000	2.91–10	—	9.19–10	1.67–15
4 000	5.27–10	—	9.49–10	4.56–15
6 000	7.34–10	5.06–18	9.77–10	1.62–14
8 000	9.21–10	1.75–16	1.00–9	4.46–14
10 000	1.09–9	1.67–15	1.02–9	9.87–14
15 000	1.47–9	4.36–14	1.07–9	3.94–13
20 000	1.79–9	2.66–13	1.10–9	9.92–13
30 000	2.33–9	1.99–12	1.16–9	3.71–12
40 000	2.78–9	6.15–12	1.20–9	9.67–12
50 000	3.18–9	1.29–11	1.24–9	1.96–11
60 000	3.53–9	2.17–11	1.28–9	3.36–11
70 000	3.85–9	3.22–11	1.32–9	5.11–11
80 000	4.14–9	4.39–11	1.27–9	7.20–11
90 000	4.40–9	5.62–11	1.41–9	9.59–11
100 000	4.66–9	6.91–11	1.46–9	1.22–10
a_1	1.07–9	4.80–13	9.90–10	2.68–15
b_1	7.88–1	1.60+1	3.93–2	1.36–1
c_1	2.93+5	1.72+3	–3.25+5	4.13+3
a_2	—	2.18–16	—	1.08–13
b_2	—	1.05+1	—	3.62
c_2	—	8.43+3	—	7.84+4

the $Si^{3+}(3s\,^2S)$, its population should be small and therefore have little effect on attempts to measure electron capture from the Si^{3+} ground state. Figure 5 shows that the $Si^{3+}(3p\,^2P^o)$ cross section is dominated by capture to the $Si^{2+}(3s3p\,^1P^o)$ state, but when above $\sim$20 eV/u, capture into the $Si^{2+}(3s3p\,^3P^o)$ state becomes the primary channel. Capture into the $Si^{2+}(3s3p\,^1P^o)$ state has no isotope dependence, but the $Si^{2+}(3s3p\,^3P^o)$ and $Si^{2+}(3s^2\,^1S)$ capture cross sections are smaller for ^{4}He targets for collision energies below $\sim$0.5 eV/u. Quantal rate coefficients for capture into $Si^{2+}(3s3p\,^1P^o)$ and $Si^{2+}(3s3p\,^3P^o)$ states for ^{4}He and ^{3}He targets are given in tables 3 and 4, respectively.

3.4. Charge transfer ionization

Cross sections for the reverse of processes (1) through (5) are given in figure 8. All of the charge transfer ionization (not to be confused with transfer ionization when one electron is captured and another is lost to the continuum) reactions, except $Si^{2+}(3s3p\,^1P^o) + He^+ \rightarrow Si^{3+}(3s\,^2S) + He$, are endoergic with zero cross sections below a few eV u^{-1}. As stated above, the cross sections of the weaker channels may be modified if rotational coupling is considered.

Rate coefficients $\alpha_i(T)$ for charge transfer ionization can be obtained from the detailed

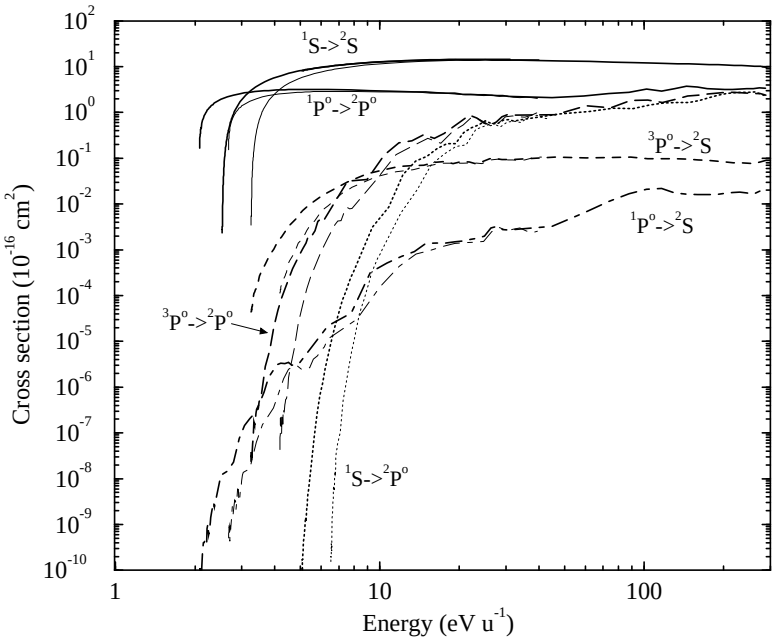

Figure 8. Charge transfer ionization cross sections, Si^{2+} + $^4He^+$($^3He^+$) $\rightarrow$ Si^{3+} + ^{4}He(^{3}He) with $^4He^+$ (thick curves) and $^3He^+$ (thin curves) targets. The initial Si^{2+} and final Si^{3+} states are indicated in the figure and the energy scale refers to the centre-of-mass collision energy in the entrance channel.

balance equation

$$\alpha_r(T) = \frac{g_f}{g_r} \exp(-\Delta E_{rf}/kT)\alpha_f(T) \tag{8}$$

where ΔE_{rf} is the asymptotic separated-atom energy defect between the reverse (ionization) and forward (charge transfer recombination) reactions, α_f the rate coefficient for charge transfer recombination reaction, and g_r and g_f the approach probability factors for the initial channel in the reverse and forward directions, respectively.

4. Astrophysical applications

Emission lines of Si III are observed in a variety of astrophysical sources including solar and stellar atmospheres (Baliunas and Butler 1980), planetary nebulae (Clegg *et al* 1987), symbiotic stars (Keenan *et al* 1992), novae (Morisset and Péquignot 1996), H II regions (Rubin *et al* 1993), and shocked regions of interstellar gas (Butler and Raymond 1980). The most prolific line is the 1883/1892 Å ($3s3p\,^3P^o \rightarrow 3s^2\,^1S$) intercombination transition which is often used as an electron density diagnostic. Reaction (1) only populates the ground state while reactions (2) and (4) have rate coefficients which are too small to significantly affect the $3s3p\,^3P^o$ population. The $3s3p\,^3P^o$ level is therefore primarily populated by electron impact excitation (Keenan *et al* 1992). However, reaction (1), as well as its reverse, can have a significant influence on the silicon ionization equilibrium which in turn was shown by Baliunas and Butler (1980) to increase the solar Si III 1892 emissivity and shift the temperature of its peak. The change in ionization balance by charge transfer was also demonstrated by Butler and Raymond (1980) to affect the emission line flux of Si III 1892 behind a shock.

5. Summary

We have presented a completely *ab initio* MOCC investigation of low-energy electron capture in collisions of Si^{3+} with atomic helium. Results for capture from the Si^{3+} ground state are in good agreement with Landau–Zener calculations and previous MOCC results, but are about 40% smaller than an ion trap measurement. Electron capture from the $Si^{3+}(3p\,^2P^o)$ excited state has been studied and target isotope effects have been addressed.

Acknowledgments

The work of PCS was performed as a Eugene P Wigner Fellow and staff member at the Oak Ridge National Laboratory, managed by Lockheed Martin Energy Research Corp for the US Department of Energy under Contract DE-AC05-96OR22464. BZ acknowledges support from the National Science Foundation through EPSCoR grant OSR-9353227 in Chemical Physics to the state of Nevada and by a grant for the Institute for Theoretical Atomic and Molecular Physics to the Smithsonian Institution and Harvard University. BZ also thanks the University of Nevada, Las Vegas sabbatical committee.

References

Baliunas S L and Butler S E 1980 *Astrophys. J. Lett.* **235** L45
Bashkin S and Stoner J O Jr 1975 *Atomic Energy-Levels and Grotrian Diagrams* (Amsterdam: North-Holland)
Butler S E and Dalgarno A 1980 *Astrophys. J.* **241** 838
Butler S E and Raymond J C 1980 *Astrophys. J.* **240** 680
Clarke N J 1995 *Doctoral Thesis* University of Liverpool
Clarke N J and Cooper D L 1998 *J. Chem. Soc. Faraday Trans.* **94** 3295
Clarke N J, Stancil P C, Zygelman B and Cooper D L 1998 *J. Phys. B: At. Mol. Opt. Phys.* **31** 533
Clegg R E S, Harrington J P, Barlow M J and Walsh J R 1987 *Astrophys. J.* **314** 551
Cooper D L, Gerratt J and Raimondi M 1988 *Int. Rev. Phys. Chem.* **7** 59
Fang Z and Kwong V H S 1997 *Astrophys. J.* **483** 527
Honvault P, Bacchus-Montabonel M C, Gargaud M and McCarroll R 1998 *Chem. Phys.* **238** 401
Johnson B R 1973 *J. Comput. Phys.* **13** 445
Keenan F P, Feibelman W A and Berrington K A 1992 *Astrophys. J.* **389** 443
Morisset C and Péquignot D 1996 *Astron. Astrophys.* **312** 135
Pieksma M, Gargaud M, McCarroll R and Havener C C 1996 *Phys. Rev.* A **54** R13
Rubin R H, Dufour R J and Walter D K 1993 *Astrophys. J.* **413** 242
Stancil P C and Zygelman B 1995 *Phys. Rev. Lett.* **75** 1495
Stancil P C, Zygelman B, Clarke N J and Cooper D L 1997a *Phys. Rev.* A **55** 1064
——1997b *J. Phys. B: At. Mol. Opt. Phys.* **30** 1013
Zygelman B, Cooper D L, Ford M J, Dalgarno A, Gerratt J and Raimondi M 1992 *Phys. Rev.* A **46** 3846